Automotive Experiences
Vol. 6 No. 1 (2023) pp. 200-215
p-ISSN: 2615-6202 e-ISSN: 2615-6636

Research Paper

Design of Metallic Catalytic Converter using Pareto Optimization to Improve Engine Performance and Exhaust Emissions

Sudirman Rizki Ariyanto, Suprayitno, Retno Wulandari

Department of Mechanical Engineering, Universitas Negeri Malang, 65145, Indonesia

suprayitno@um.ac.id

https://doi.org/10.31603/ae.7977

Check for updates

Published by Automotive Laboratory of Universitas Muhammadiyah Magelang collaboration with Association of Indonesian Vocational Educators (AIVE)

Article Info
Submitted:
02/10/2022
Revised:
11/04/2023
Accepted:
15/04/2023
Online first:
28/04/2023

Abstract

In this paper, Metallic Catalytic Converter (MCC) is installed in motorcycle exhausts to produce the minimum CO as well as to produce the optimum engine power. The results from previous research were collected and then used to predict the best MCC design using the Artificial Neural Network-Multiobjective Genetic Algorithm (ANN-MOGA). In addition, the ANN parameter tuning process was also carried out using the Taguchi method to find the initial weighting and bias that is able to provide the best and the most stable performance to predict the best MCC design. The best two sets of design solutions out of 70 sets of Pareto solutions were obtained by ANN-MOGA. Those two MCC designs are the optimum emission design and the optimum multiobjective design. The verification results show that the optimum multiobjective design tends to be superior in terms of CO emissions and engine power. In terms of CO emissions, the optimum multiobjective design gets a larger S/N ratio of -10.98, while the optimum emission design only gets an S/N ratio of -11.21. Meanwhile, in terms of engine power, the optimum multiobjective design gets a larger S/N ratio of 16.13, while the optimum emission design only gets an S/N ratio of 15.86 S/N. It is in line with the ANOVA test results which show that the optimum multiobjective design is proven to be better than the optimum emission design.

Keywords: Metallic Catalytic Converter; Pareto solutions; Artificial Neural Network; Genetic Algorithm; CO Emission; Engine Performance

1. Introduction

Along with the increasing number of motorized vehicles, especially motorbikes, fuel consumption and tailpipe emissions have become an ongoing discussion by stakeholders and researchers [1]–[3]. Therefore, global and local emission standards are increasingly stringent, especially in limiting carbon monoxide (CO) and hydrocarbons (HC) from exhaust pipes. In Indonesia, motor vehicle emissions are regulated in the Minister of Environment Regulation No. 5 of 2006. It was stipulated that CO and HC emissions allowed were 5.5% and 2400 ppm by volume for motorcycles produced until 2010. Meanwhile, CO and HC emissions allowed were each 4.5% and 2000 ppm volume for motorcycles manufactured after 2010. CO and HC can be reduced by the application of alternative fuels, the addition of a mixture control device, as well as modification of engine components [4]–[10]. CO and HC emissions at the exhaust end can also be reduced by the application of Metallic Catalytic Converter (MCC). This technology works by oxidizing CO emissions to CO_2 and HC emissions to H_2O [11]. Thus, exhaust emissions from the exhaust end become more environmentally friendly.

Currently, the MCC used by automotive manufacturers is made of platinum group metal (PGM). This material was effective to decrease emissions up to 85–90% for CO and HC at 250 °C and up to 100% NOx at 400 °C [12]–[14]. Unfortunately, this material also has some weaknesses, for example in production costs and

availability of the raw material [15]. Therefore, further development of MCC is carried out by using alternative materials that have similar characteristics to PGM [16]. Some works are focused on optimizing the MCC configuration, from the use of mono, dual, and three-way designs to minimizing exhaust emissions. Until now, the three-way catalytic converter is mostly used in MCC applications [17].

Functionally, MCC was created to reduce exhaust emissions from motorized vehicles, especially gasoline engines. However, the use of MCC is also reported to have an impact on engine performance. Prabhahar *et al*. [18] reported that the use of copper in the MCC was quite effective in the oxidation process of CO and HC emissions and increased engine performance which was affected by the inlet and outlet angles of the MCC casing. According to Bell theory [19], the inlet and outlet angles of the MCC casing are designed to optimize exhaust flow by minimizing back pressure. Bhure [20] reported that the higher the back pressure, the lower the engine performance. Other researchers claim that using MCC with copper material coated with titanium dioxide (TiO_2) can increase torque by 7.15% and power by 6.13% [21]. Furthermore, Ellyanie & Oktabri [22] proved that the brass catalytic converter increased engine efficiency by around 17.65%.

Based on previous studies, it is known that the process of finding the best MCC design is carried out through experimental research which is relatively expensive and requires a long time. Therefore, referring to previous MCC research data, we chose the optimization method with Artificial Neural Network-Multiobjective Genetic Algorithm (ANN-MOGA) to predict the best MCC design. In this study, ANN was chosen because of its ability to accommodate complex non-linear data with multiple inputs [23], [24]. It is known that data from previous research is not well patterned, as well as from various configurations, types of materials, and vehicles. Furthermore, in this study there are six MCC configuration parameters used as input data with two output parameters.

This research also uses MOGA as the search engine for the MCC parameters combinations. It is called multiobjective or Pareto optimization because it is different from single-objective optimization. Pareto optimization solves problems involving two or more objectives that are contradicted each other [25]. In this case, two objectives to be optimized simultaneously are CO emissions and power. These goals contradict each other, where by implementing MCC it is expected to produce the CO as low as possible and produce the engine power as much as possible [26]. Meanwhile, the use of genetic algorithms is known to be very powerful, efficient, and well known to have a small probability of being trapped in the local optimum [27]. The ANN-MOGA optimization of the MCC design is the original contribution of this paper. This work shows some of the best design solutions of MCC that do not outperform each other (also known as frontier Pareto solutions or Pareto solutions or non-dominant solutions) and can be selected according to needs in the use of MCC.

2. Methods

2.1. Data Sets

This research uses the data set obtained from previous collaborative works [28]–[34]. From these works, a total of 231 data sets representing different MCC designs under various engine operating rotational speeds were collected based on six design variables. The six design variables which are also the ANN input parameters are (1) material (Mtl); (2) curve height (CH); (3) tube length (TL); (4) tube diameter (TD); (5) input angle (IA); and (6) output angle (OA) as shown in Figure 1. The determination of the MCC variable was chosen based on similarities from several previous studies. In this case, the material is the main reference while several previous studies used more than three types of materials from alternative metal groups such as copper, chrome-plated copper, and brass.

The variables referred to hereinafter related to efforts to obtain the largest possible surface area by modifying the indentation height, tube length, tube diameter, inlet angle, and outlet angle of the MCC. According to the Bernard study [35], the specific surface area of the catalyst greatly influences the efforts to accelerate the catalytic reaction rate. In this case, the MCC performance is measured from the level of CO emissions and engine power. The selection of CO emissions and engine power as indicators in determining MCC

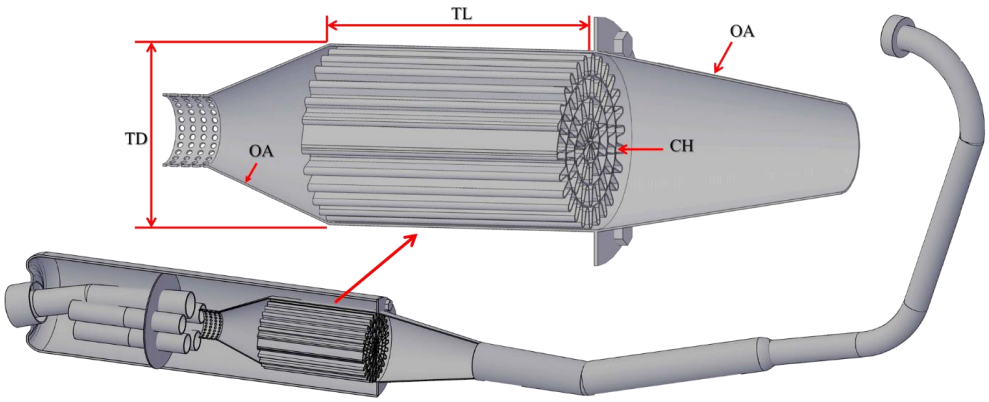

Figure 1. MCC construction on exhaust system

performance is based on the similarity of the trends of the two variables. When CO emissions increase, it is certain that the HC emissions also increase. As well as when engine power increases, it is certain that engine torque increases. Considering those facts, in the design optimization process, MCC performance is measured from CO exhaust emission levels and engine power. The 231 data sets were then used to train the ANN to map the six design variables to two output MCC performances.

2.2. *Optimization Process*

ANN have extraordinary abilities in predicting, classifying, and matching real data and can be adjusted according to needs. For example, to process non-linear data, it is highly recommended to use a three-layer neural network or what is commonly called a multilayer perceptron (MLP) [36]. The three layers include the input layer, the hidden layer, and the output layer [37]. The selection of the input variables is based on the variables that affect the output variable - decreasing CO emissions and increasing power. Based on the literature study and the results of previous studies, it is known that there are six influential variables as described in the sub-data set. Meanwhile, the combination of hidden layer and neuron parameters is obtained through the ANN parameter tuning process using the Taguchi method with a signal-to-noise (S/N) ratio approach.

Signal-to-noise ratio (S/N) is a logarithmic function that is used to optimize the product of each parameter and analyze the parameter variations [26]. Good or bad product quality depends on the S/N ratio category used. For example, smaller the Better (STB), Larger the Better (LTB), or Nominal the Best (NTB) [38]. Mitra *et al.* [39] states that the use of the Taguchi method is more effective if it is used to optimize the mean and minimize the standard deviation, which refers to the use of the S/N ratio type smaller the better (Eq. 1). It is expected that the noise or error generated is relatively small. So, it shows the stability of the initial weighting and bias [40]. However, we need to keep in mind that regardless of the characteristics or type of S/N ratio chosen, the interpretation always leads to the larger the better type. It means that the smaller the mean and standard deviation and the greater the value of the S/N ratio, the better [41].

$$S/N_{STB} = -10 \cdot \log_{10}\left(\frac{1}{n}\sum_{i=1}^{n} y_i^2\right) \quad (1)$$

$$S/N_{LTB} = -10 \cdot \log_{10}\left(\frac{1}{n}\sum_{i=1}^{n}\left(\frac{1}{y_i^2}\right)\right) \quad (2)$$

where, n is the number of trials, while y^2i is the measurement value [42]. The tuning results show that the MCC ANN structure can work optimally when using the combination of hidden layer parameters and neurons of three layers and seven neurons, respectively. Meanwhile, the transfer function hidden layer and output layer respectively use sigmoid log and tan sigmoid with Levenberg-Marquadt as learning algorithm (from previous result). In detail, the ANN structure is presented in **Figure 2**.

After the ANN structure parameter combination has been found, the next step is to compile the ANN modeling structure coding. Coding that has been compiled is then executed, where the running process from the previously

provided dataset (231 variations of the MCC design) is divided randomly into three partitions, namely training data, validation data, and testing data. Alaloul [43] explains that the training step is a crucial process in constructing ANN. 70% of the 231 data set was used as training data, while 15% as validation data to avoid overfitting ANN learning process [44]. The rest of the 15% data was then used as the testing data to evaluate the ANN accuracy. Training, validating, and testing data were randomly selected from 231 data sets [24].

The performance of ANN modeling can be measured based on the error shown by the output. The smaller the error generated, the more optimal the ANN modeling performance. If the error value generated is relatively large, the predicted value generated is certainly not accurate. So, improvements need to be made [45]. In this case, the improvement can be divided into two solutions, where the first solution is to increase the amount of data entered in the dataset, while the second solution is to retune the ANN structure using a different method. This process can be repeated so that ANN modeling can produce accurate predictive values to be continued in the verification process.

The next process after the ANN modeling is completed is compiling a MOGA coding. In this case, MOGA is used considering its advantages as a search engine for a combination of parameters that is strong and efficient. It is also not easily trapped in the local optimum [46]. MOGA optimization is specifically carried out to find a combination of input variables from the MCC that can provide a small value of CO emissions with a large power value. The MOGA optimization stages can be visualized as shown in **Figure 3**.

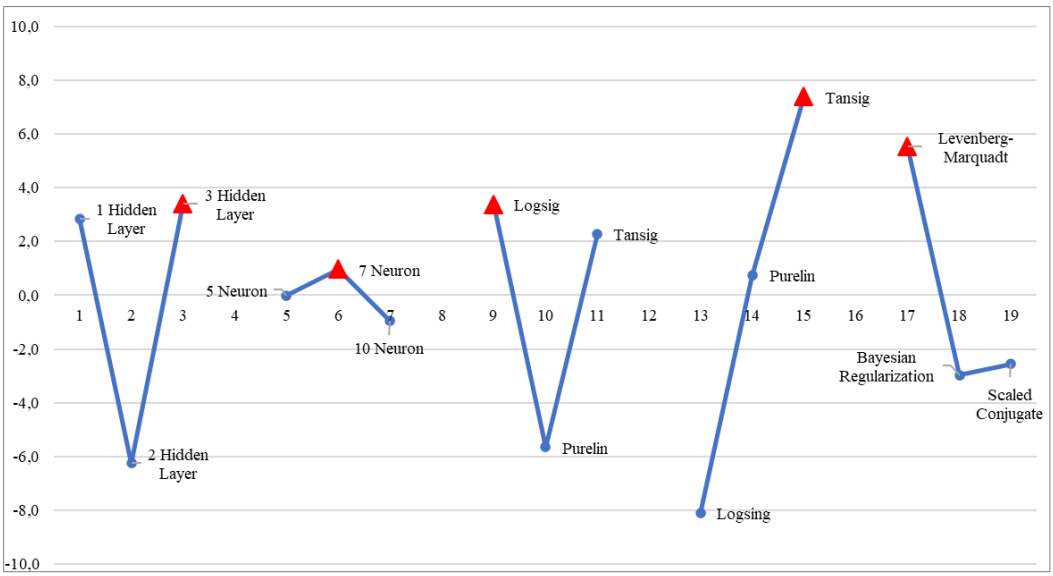

Figure 2. MCC effect plot to S/N ratio

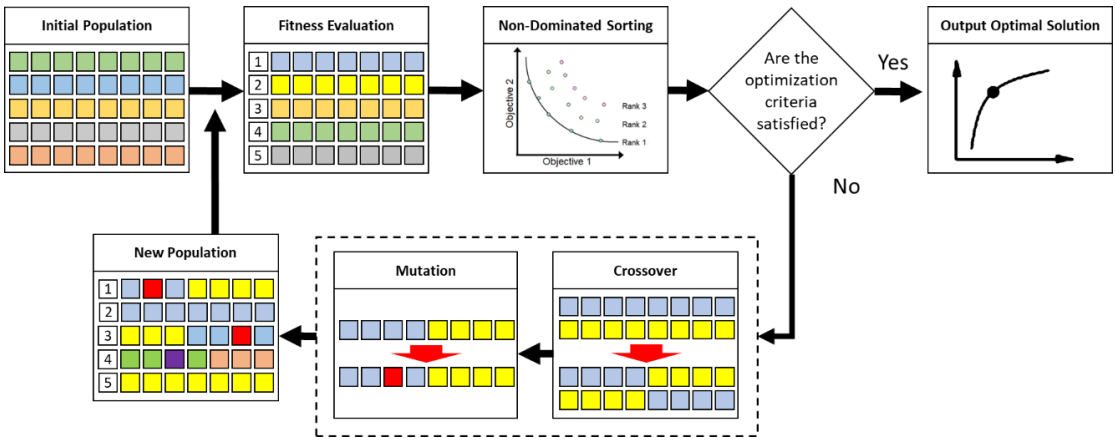

Figure 3. MOGA optimization stages

In the initial population and fitness evaluation stages, the initial population was collected through the results of previous MCC studies based on six MCC parameters, which were then measured for their fitness evaluation values. The next stage is parent selection which is intended to get some of the best parent pairs which will then enter the crossover stage [47]. The Crossover is done by mating the two individuals to get a new individual. This process is carried out by exchanging several combinations of the first parent's MCC variables with combinations of MCC variables from the second parent [48]. After the crossover process is carried out, the mutation process is continued. The mutation process in this study was carried out on one or more MCC variables in order to prevent the population from having variables that were too similar to each other [49].

At the mutation stage, a new individual is obtained with a different combination of MCC variables from the previous individual. The new individual is then tested for fitness through the ANN modeling structure that has been built. From the ANN modeling, it is possible to know the predictions of the CO and HC values that will be obtained. After several new individuals have been tested for fitness, the next step is population selection. Population selection is based on some of the best parents, which is grouped with new individuals who have predicted CO and its power. Individuals in the new generation will survive (not be eliminated) if they produce CO and better power than the previous generation, and vice versa [50].

Another goal that needs to be optimized simultaneously in this research is CO emissions and power. These goals are of course contradictory to each other, whereby applying MCC it is hoped that the CO value is as small as possible, and the power value is as large as possible. Therefore, there is no single solution from MCC that can be considered optimal. However, in this research, we will obtain a set of optimal solutions known as non-dominated solutions or Pareto optimal solutions or Pareto fronts [26]. The optimum point of a set of optimal solutions obtained will be shown along the lines or points of the Pareto front graph.

2.3. *Instruments for Verification*

The research tools and instruments used in this study is presented in **Figure 4** and their specification is presented in **Table 1**. In addition, the data collection process for backpressure on the muffler is also carried out. It aims to measure how much exhaust gas pressure is trying to return to the combustion chamber before and after using the MCC [51]. Back pressure measurements were carried out using a U-tube manometer (**Figure 5**) and calculated by the Eq. (3), where ΔP is pressure difference, ρ is density, g is gravitational acceleration, and is h liquid level [52].

$$\Delta P = \rho\, g\, h \tag{3}$$

Figure 4. Research instruments

Table 1. Specifications for research equipment and instruments

No	Specification	Chassis Dynamometer	Exhaust Gas Analyzer	Blower
1.	Brand	Rextor Pro-Dyno	Heshbon HG-520	Krisbow
2.	Voltage	220 V 50/60 Hz	220/240Vac 50/60Hz	230 V, 7.60 A
3.	Operation range	6.000 rpm with 150 gears	0-9.99% with 0.01% resolution	1200 rpm

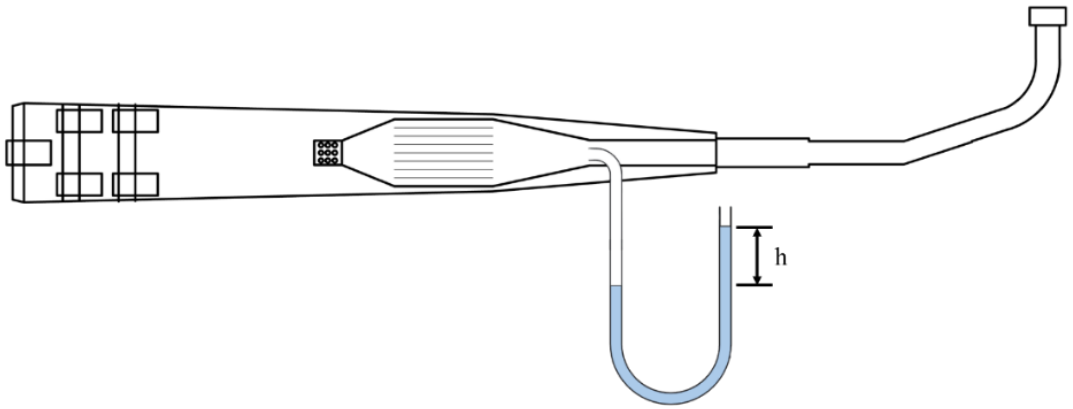

Figure 5. Illustration of back pressure measurement

Data collection was carried out in the Mechanical Performance Testing Laboratory, Department of Mechanical Engineering, Faculty of Engineering, Universitas Negeri Surabaya. The research equipment and instruments used are shown in **Figure 4**. In addition, in the process of obtaining valid and reliable research data, CO emission and power testing are carried out based on national and international standards. The measurement of motorcycle exhaust emissions is based on SNI 09-7118.2 [53], while the measurement of engine performance is based on SAE J1349 [54].

3. Results and Discussion

3.1. ANN-MOGA Optimization Results

The database used in the ANN-MOGA optimization process is data from previous studies with similar input variables. ANN-MOGA coding works by studying and recognizing previous research data patterns which are then used to predict the combination of MCC variables with the smallest possible CO emission value and the largest possible vehicle power. Through this interface (**Figure 6**), we can ensure that the structure of the ANN is in accordance with the results of the ANN parameter tuning. After showing the interface structure of the ANN from nntraintool, then the Pareto front interface diagram appears to show the process of finding the best MCC design as shown in **Figure 7**.

From **Figure 7**, we can see that there are two main objectives that are used as benchmarks in determining the best design - CO emissions and power. The optimal points based on the two obejectives are distributed along the points of the Pareto optimal graph. This point is then more commonly known as the set of trade-off optimal solutions or Pareto optimal solutions or Pareto fronts [26]. In this case, if one set of solutions in the diagram is presented in the form of design variations, then there are 70 sets of MCC design solutions that do not dominate each other. The meaning of not dominating each other is certainly related to the compromise value that is in accordance with the optimization objectives without reducing the ability of one of the output variables [55], [56]. Furthermore, the 70 sets of solutions were analyzed in greater depth through equal weighting. As a result, two sets of the best design solutions were found as shown in **Table 2**.

Based on the results, the two optimum design sets were selected from the 70 design solutions sets. These designs include MCC Design 37, which is the design with the smallest CO emission value, and MCC Design 39, which is a design that considers the smallest possible CO emission value with the most significant possible power value. MCC Design 37 is hereinafter referred to as optimum emission design while MCC Design 39 is referred to as optimum multiobjective design. The two designs were then tested experimentally.

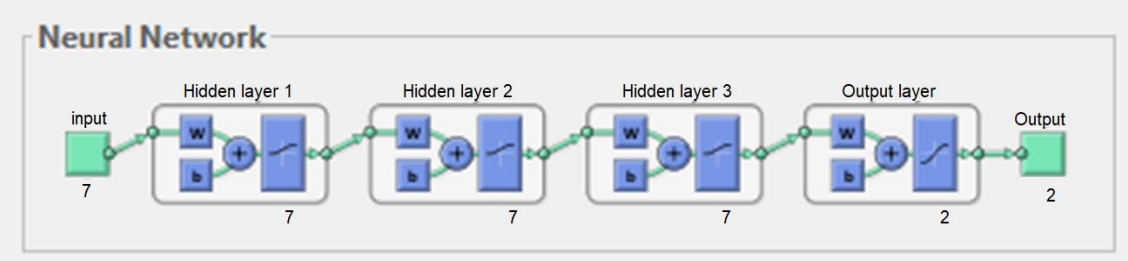

Figure 6. Interface neural network training

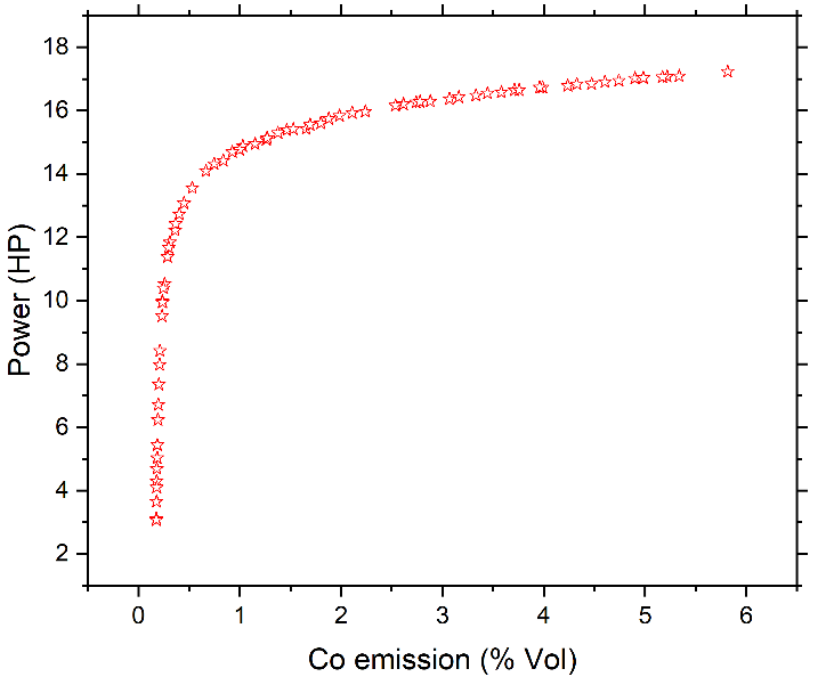

Figure 7. Pareto optimal solutions

Table 2. Test results on ANN-MOGA output

MCC	Material	CH (mm)	TD (mm)	TL (mm)	IA (°)	OA (°)	Engine speed (rpm)	CO (%Vol)	Power (HP)
Optimum emission design	CuCr	2.8	63.1	70.5	12	14	9249	0.18	3.1
Optimum multiobjective design	CuCr	3.5	60.8	88.1	12	22	9302	0.53	13.5

3.2. *Experimental Verification Results*

Experimental testing of optimum emission design and optimum multiobjective design was carried out to test the actual value of CO emissions and the resulting vehicle power. The optimum emission design and optimum

multiobjective design MCC fabrication results are presented in **Figure 8**. Tests were carried out on three different types of vehicles (**Figure 4**), where each vehicle represented a type of sport, automatic, and moped.

Referring to the prediction results of ANN-MOGA, it is known that the value of CO emission and the best vehicle power from the optimum emission design is produced at 9249 rpm. Meanwhile, the optimum multiobjective design was found at 9302 rpm. The two engine speed values will certainly be difficult to obtain under actual test conditions, so in this study, the comparison of test results was carried out at 9000 rpm. The comparison results are shown in **Table 3**.

Referring to the results of the S/N ratio calculation based on testing at 9000 rpm (**Table 3**), it is known that the optimum emission design gets an S/N ratio calculation value of -11.35 while the optimum multiobjective design gets the calculation value of the S/N ratio of -10.32. The calculation of the S/N ratio on the CO emission test results uses the smaller the better type, which means the smaller the mean and standard deviation values, and the larger the S/N ratio, the better (Eq. 1) [41]. Therefore, from these two values, we can observe that the optimum multiobjective design produces an S/N ratio value that is greater than the optimum emission design. That is, based on the results of experimental verification, the optimum multiobjective design tends to produce lower CO emissions than the optimum emission design.

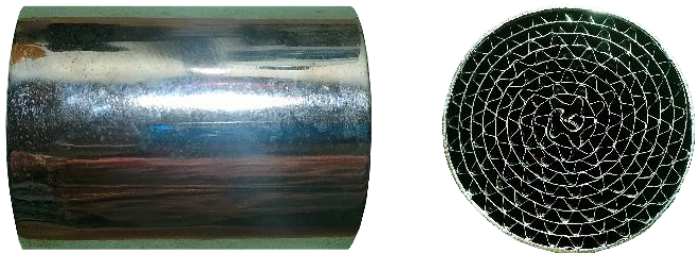

(a)

(b)

Figure 8. MCC designed: (a) optimum emission design and (b) optimum multiobjective design

Table 3. Comparison S/N ratio at 9000 rpm

MCC	Mean		STDEV		S/N Ratio	
	CO	Power	CO	Power	CO	Power
Optimum emission design	2.46	8.50	2.76	4.59	-11.35	15.86
Optimum multiobjective design	2.14	8.60	2.49	4.44	-10.32	16.13

In line with the results of the CO emission test, the results of the vehicle power test also show that the optimum multiobjective design tends to be better than the optimum emission design. It is evidenced by the results of the S/N ratio calculation based on laboratory

scale testing. Optimum emission design gets an S/N ratio calculation value of 15.86 while the optimum multiobjective design gets an S/N ratio calculation value of 16.13. The calculation of the S/N ratio on the results of the vehicle power test uses the larger the better type, which means the smaller the standard deviation value, the greater the mean value, and the better S/N ratio (Eq. 2) [57]. From these two values, we can observe that the optimum multiobjective design produces an S/N ratio value that is greater than the optimum emission design. Based on the results of experimental verification, the optimum multiobjective design tends to produce greater vehicle power than the optimum emission design.

Experimental testing was carried out on both MCC designs using three different types of motors and tested at different engine speed. Analysis of variance (ANOVA) was carried out on these three variables, both for CO emissions and engine power with a significance level, α=0.05. Analysis of variance on the motor types and rotation variation is used to block the effect of the two variables. The three types of motorbikes are Yamaha Vixion, Honda Vario and Honda Supra. There are 9 levels of engine speed for testing CO emissions starting from 1500 rpm (idle) to 9000 rpm in multiples of 1000 rpm. Meanwhile, for engine power testing, there are 14 levels of engine speed from 3000 rpm to 9500 rpm in multiples of 500 rpm. The engine power measurement starts from 3000 rpm, this is based on the output data that comes out of the dynamometer chassis software starting from that rotation.

For CO emission, the ANOVA results show a significance of 0.102, which is greater than the significance level of α=0.05 to accept the null hypothesis (H0), as shown in **Table 4**. Thus, the two MCC designs do not differ significantly in terms of CO emissions. However, the ANOVA results for the engine power in the two MCC designs show a significance level of 0.017 (**Table 5**). Thus, the two MCC designs differ significantly in engine power. The MCC design with Pareto optimization results is better in terms of mechanical power performance than the MCC design with the best CO performance, as shown in **Table 3**.

Further analysis was carried out to reveal the reasons why the optimum multiobjective design has a superior tendency in terms of reducing CO emissions. One of the main reasons is that the optimum multiobjective design uses chrome-plated copper, which is

Table 4. ANOVA for CO emmissions

Source	Type III Sum of Squares	df	Mean Square	F	Sig.
MCC_Design	2.015	1	2.015	2.871	0.102
Motorcycle_Type	54.201	2	27.101	38.625	0.000
Rpm_Engine	37.946	8	4.743	6.76	0.000
Error	18.243	26	0.702		
Total	887.396	54			

Table 5. ANOVA for engine power

Source	Type III Sum of Squares	df	Mean Square	F	Sig.
MCC_Design	0.252	1	0.252	6.192	0.017
Motorcycle_Type	404.412	2	202.206	4970	0.000
Rpm_Engine	188.852	13	14.527	357.061	0.000
Error	1.668	41	0.041		
Total	5210.74	84			

the second-best oxidation and reduction catalyst after Manganese (Mn) for transition metals [12]. Azri *et al*. [58] identified a sequence of several metals that are known to be effective as oxidation and reduction catalysts including Pt, Pd, Ru > Mn, Cu > Ni >

Fe > Cr > Zn, and the oxides of these metals. Supporting this, Li *et al*. [59] suggested that copper (Cu) is one of the most effective transition metal materials when used as a catalyst.

Other facts were also found related to the tendency of the optimum multiobjective design, which excels in reducing CO emissions including the relatively longer length of the MCC tube, which is 88.1 mm with an indentation height of 3.5 mm, and the MCC tube diameter of 60.8 mm. Besides, the output angle of the optimum multiobjective design casing tends to be steeper than the optimum emission design. This allows the flue gas stream to tend to collect in the MCC casing area and causes increased oxidation activity between the MCC surface and the exhaust gas.

In accordance with the results of the experimental tests above, we can see that MCC has an important role in the oxidation process of CO emissions. The oxidation process from CO to CO_2 is influenced not only by the surface area of the MCC that is in contact with the exhaust gas, but also by the temperature factor. As we know from the kinetic theory of gases, the kinetic energy of gases is directly proportional to temperature [60]. As the temperature increases, the molecules gain energy and move faster so that the number of effective collisions increases as illustrated in **Figure 9**. The increase in the number of effective collisions is also directly proportional to the reaction rate [61]. In this case, the use of MCC plays an important role in the process of accelerating the reaction rate by lowering the activation energy.

Through the use of MCC optimum multiobjective design, the oxidation process can occur faster, namely at a temperature of 575 °C in all types of vehicles. Thus, the oxidation process of CO + ½ O_2 emissions to CO_2 can already be processed even though it occurs at a lower temperature. In the process, the oxidation reaction begins with the adsorption process (binding) of CO and CO_2 emissions on the MCC surface [62]. The O_2 molecule becomes isolated into two O atoms. The adsorbed O atoms and the adsorbed CO molecules then react on the surface of the MCC optimum multiobjective design to form CO_2. Then the resulting CO_2 product is desorbed (removed) so that CO_2 emissions can come out of the MCC surface [63]. Thus, the MCC surface can carry out further oxidation reactions. In more detail, an illustration of the oxidation process of CO emissions can be seen in **Figure 10**.

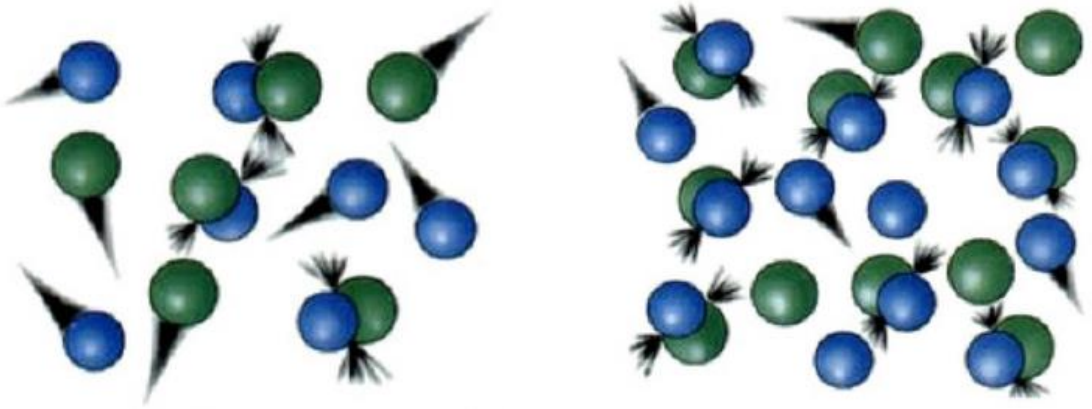

(a) (b)

Figure 9. Kinetic energy at (a) low temperature and (b) high temperature [61]

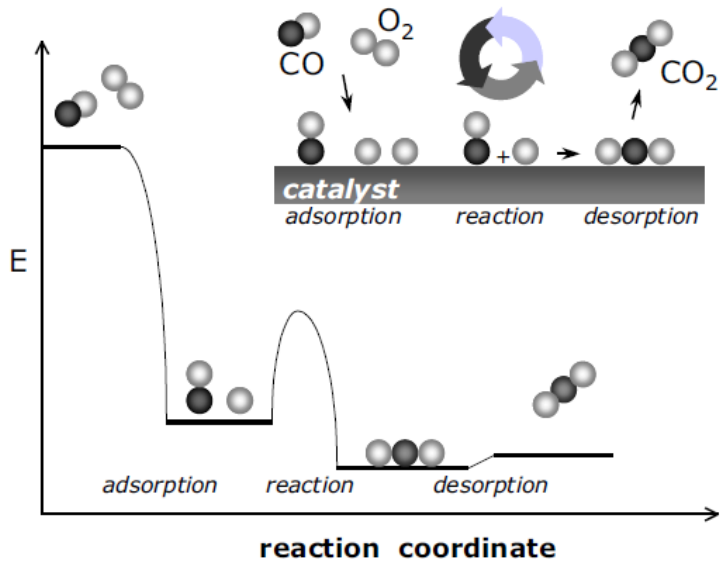

Figure 10. Reaction cycle and process diagram of CO oxidation to CO_2 [63]

Dey & Mehta [64] explains that the rate of catalytic oxidation depends on the surface area of the catalyst. The larger the surface area and the more exhaust gases that are in contact with the catalyst surface, the more CO and HC emissions are oxidized to CO_2 and H_2O [60]. In this case, the use of chrome plated copper as MCC material is the right choice because this material has corrosion resistance and is able to withstand high temperatures [65]. As the temperature increases, the molecules gain energy and move faster so the number of effective collisions increases. The increasing number of effective collisions is directly proportional to the reaction rate [61]. In this case, the use of MCC plays an important role in the process of accelerating the reaction rate by lowering the activation energy so that the oxidation process can occur faster at a temperature of +500 °C.

In terms of power, emission-optimized designs tend to be superior to multiobjective-optimal designs. The optimal emission design gets an S/N ratio calculation value of 15.62 while the optimum multiobjective design gets an S/N ratio calculation value of 15.59. This shows that when viewed from testing at each engine speed the optimum emission design tends to produce greater vehicle power than the optimum multiobjective design. The increase in power occurs, of course, not because of the MCC material, but because of the difference in the MCC casing design.

The optimum emission design casing is set with an inlet angle of 12° with an outlet shrinkage of 14°, while the optimum multiobjective design casing is set with an inlet angle of 12° and an outlet angle of 22°. Referring to the two casing designs, it is known that the outlet angle of the optimum multiobjective design casing tends to be steeper when compared to the optimum emission design casing. In accordance with the theory proposed by Bell [19], it is known that the outlet angle which tends to be steeper (22°) allows the exhaust gas flow to be obstructed and collected in the MCC casing area. Moreover, the turbulence that occurs tends to be large and causes the exhaust gas to lose flow [66].

This condition certainly causes an increase in exhaust gas pressure which leads back to the combustion chamber when overlapping. This has an impact on the decreasing power of the vehicle because the exhaust gases cannot freely exit the environment. Furthermore, to prove this, the back pressure measurement is carried out in the exhaust. The results show that the back pressure

generated by the optimum emission design is 0.52 kPa, while the back pressure generated by the optimum multiobjective design tends to be lower at 0.41 kPa.

4. Conclusion

From this study, the pattern of previous research data is used to predict the best design of MCC by ANN-MOGA. The design variables are material, indentation height, diameter, length, angle in, and angle out of the MCC. Based on the data and coding, the optimum emission design and optimum multiobjective design were found. The verification results show that the optimum multiobjective tends to be superior both in terms of CO emissions and engine power. The optimum multiobjective design produces lower CO emissions with an S/N ratio value of -10.98, while the optimum emission design produces CO emissions with an S/N ratio value of -11.21. Meanwhile, in terms of vehicle power, the optimum multiobjective design produces greater vehicle power with an S/N ratio value of 16.13, while the optimum emission design produces vehicle power with an S/N ratio value of 15.86. It is in line with the results of the ANOVA test which shows that the optimum multiobjective design is proven to be better than the optimum emission design.

Author's Declaration

Authors' contributions and responsibilities

The authors made substantial contributions to the conception and design of the study. The authors took responsibility for data analysis, interpretation and discussion of results. The authors read and approved the final manuscript.

Funding

This research is funded by LP2M Universitas Negeri Malang for the 2022 funding year.

Availability of data and materials

All data are available from the authors.

Competing interests

The authors declare no competing interest.

Additional information

No additional information from the authors.

References

[1] J.-H. Tsai, Y.-C. Yao, P.-H. Huang, and H.-L. Chiang, "Fuel economy and volatile organic compound exhaust emission for motorcycles with various running mileages," *Aerosol and Air Quality Research*, vol. 18, no. 12, pp. 3056–3067, 2018, doi: 10.4209/aaqr.2018.07.0264.

[2] O. A. Odunlami, O. K. Oderinde, F. A. Akeredolu, J. A. Sonibare, O. R. Obanla, and M. E. Ojewumi, "The effect of air-fuel ratio on tailpipe exhaust emission of motorcycles," *Fuel Communications*, vol. 11, p. 100040, 2022, doi: 10.1016/j.jfueco.2021.100040.

[3] Y.-L. T. Nguyen, A.-T. Le, K. N. Duc, V. N. Duy, and C. D. Nguyen, "A study on emission and fuel consumption of motorcycles in idle mode and the impacts on air quality in Hanoi, Vietnam," *International Journal of Urban Sciences*, vol. 25, no. 4, pp. 522–541, 2021, doi: 10.1080/12265934.2020.1871059.

[4] R. Anggrainy, W. Ruslan, D. L. Zariatin, R. A. Gilart, and T. Syam, "Effect of gasoline vaporizer tube (GVT) with magnetic field on spark-ignition engine: Investigation, discussion, and opinion," *Mechanical Engineering for Society and Industry*, vol. 2, no. 2, pp. 98–106, 2022, doi: 10.31603/mesi.7075.

[5] L. M. Olalekan, O. Olatunde, F. I. Olufemi, and A. A. Olamide, "Mathematical modeling and cost comparison for electricity generation from petrol and liquified petroleum gas (LPG)," *Mechanical Engineering for Society and Industry*, vol. 2, no. 2, pp. 56–62, 2022, doi: 10.31603/mesi.6697.

[6] B. Waluyo and B. C. Purnomo, "Exhaust Gas Emissions of Homogeneous Gasoline-Methanol-(Ethanol) Blends," *Automotive Experiences*, vol. 5, no. 2, pp. 173–181, 2022, doi: 10.31603/ae.6599.

[7] T. Dinh, K. Nguyen, T. Pham, and V. Nguyen, "Study on performance enhancement and emission reduction of used carburetor motorcycles fueled by flex-fuel gasoline-ethanol blends," *Journal of the Chinese Institute of Engineers*, vol. 43, no. 5, pp. 477–488, 2020, doi: 10.1080/02533839.2020.1751719.

[8] T. Dinh Xuan, D. Vu Minh, B. P. Hoa, K. N. Duc, and V. Nguyen Duy, "Influence of

ethanol-gasoline blended fuel on performance and emission characteristics of the test motorcycle engine," *Journal of the Air & Waste Management Association*, vol. 72, no. 8, pp. 895–904, 2022, doi: 10.1080/10962247.2022.2064003.

[9] V. N. Duy, K. N. Duc, and N. C. Van, "Real-time driving cycle measurements of fuel consumption and pollutant emissions of a bi-fuel LPG-gasoline motorcycle," *Energy Conversion and Management: X*, vol. 12, p. 100135, 2021, doi: 10.1016/j.ecmx.2021.100135.

[10] V. N. Duy, K. N. Duc, D. N. Cong, H. N. Xa, and T. Le Anh, "Experimental study on improving performance and emission characteristics of used motorcycle fueled with ethanol by exhaust gas heating transfer system," *Energy for Sustainable Development*, vol. 51, pp. 56–62, 2019, doi: 10.1016/j.esd.2019.05.006.

[11] M. Real, R. Hedinger, B. Pla, and C. Onder, "Modelling three-way catalytic converter oriented to engine cold-start conditions," *International Journal of Engine Research*, p. 146808741985314, May 2019, doi: 10.1177/1468087419853145.

[12] S. K. Haldar, *Platinum-Nickel-Chromium Deposits*. Elsevier, 2016.

[13] M. Pacella *et al.*, "PGM-free CuO/LaCoO3 nanocomposites: New opportunities for TWC application," *Applied Catalysis B: Environmental*, vol. 227, pp. 446–458, Jul. 2018, doi: 10.1016/j.apcatb.2018.01.053.

[14] I. Yakoumis, E. Polyzou, and A. M. Moschovi, "PROMETHEUS: A Copper-Based Polymetallic Catalyst for Automotive Applications. Part II: Catalytic Efficiency an Endurance as Compared with Original Catalysts," *Materials*, vol. 14, no. 9, p. 2226, Apr. 2021, doi: 10.3390/ma14092226.

[15] Warju, *Teknologi Reduksi Emisi Gas Buang Kendaraan Bermotor*. Surabaya: Unesa University Press, 2013.

[16] P. Lang, N. Yuan, Q. Jiang, Y. Zhang, and J. Tang, "Recent Advances and Prospects of Metal-Based Catalysts for Oxygen Reduction Reaction," *Energy Technology*, vol. 8, no. 3, p. 1900984, Mar. 2020, doi: 10.1002/ente.201900984.

[17] E. Kritsanaviparkporn, F. M. Baena-Moreno, and T. R. Reina, "Catalytic Converters for Vehicle Exhaust: Fundamental Aspects and Technology Overview for Newcomers to the Field," *Chemistry*, vol. 3, no. 2, pp. 630–646, May 2021, doi: 10.3390/chemistry3020044.

[18] M. Prabhahar *et al.*, "Copper Oxide Nanoparticles Incorporated in the Metal Mesh Used to Enhance the Heat Transfer Performance of the Catalytic Converter and to Reduce Emission," *Journal of Nanomaterials*, vol. 2022, pp. 1–9, Jul. 2022, doi: 10.1155/2022/9169713.

[19] A. G. Bell, *Modern Engine Tuning*. Haynes Publishing, 1997.

[20] S. Bhure, "Effect of Exhaust Back Pressure on Performance and Emission Characteristics of Diesel Engine Equipped with Diesel Oxidation Catalyst and Exhaust Gas Recirculation," *International Journal of Vehicle Structures and Systems*, vol. 10, no. 3, Aug. 2018, doi: 10.4273/ijvss.10.3.09.

[21] W. Warju, N. S. Drastiawati, S. R. Ariyanto, and M. Nurtanto, "The effect of Titanium Dioxide (TiO2) based metallic catalytic converter on the four-stroke motorcycle engine performance," *Journal of Physics: Conference Series*, vol. 1747, no. 1, p. 012031, Feb. 2021, doi: 10.1088/1742-6596/1747/1/012031.

[22] E. Ellyanie and D. Oktabri H, "The Effect of Brass (Cu-Zn) Catalytic Converter Muffler On Engine Performance," *Indonesian Journal of Engineering and Science*, vol. 2, no. 2, pp. 035–043, Jul. 2021, doi: 10.51630/ijes.v2i2.20.

[23] S. S. Miriyala, V. R. Subramanian, and K. Mitra, "TRANSFORM-ANN for online optimization of complex industrial processes: Casting process as case study," *European Journal of Operational Research*, vol. 264, no. 1, pp. 294–309, Jan. 2018, doi: 10.1016/j.ejor.2017.05.026.

[24] A. Hijazi, S. Al-Dahidi, and S. Altarazi, "A Novel Assisted Artificial Neural Network Modeling Approach for Improved Accuracy Using Small Datasets: Application in Residual Strength Evaluation of Panels with Multiple Site Damage Cracks," *Applied Sciences*, vol. 10, no. 22, p. 8255, Nov. 2020, doi: 10.3390/app10228255.

[25] P. Ngatchou, A. Zarei, and A. El-Sharkawi, "Pareto Multi Objective Optimization," in *Proceedings of the 13th International Conference on, Intelligent Systems Application to Power Systems*, pp. 84–91, doi: 10.1109/ISAP.2005.1599245.

[26] M. Akbari, P. Asadi, M. K. Besharati Givi, and G. Khodabandehlouie, "Artificial neural network and optimization," in *Advances in Friction-Stir Welding and Processing*, Elsevier, 2014, pp. 543–599.

[27] K. Agbele, A. Adesina, D. Ekong, and O. Ayangbekun, "State-of-the-Art Review on Relevance of Genetic Algorithm to Internet Web Search," *Applied Computational Intelligence and Soft Computing*, vol. 2012, pp. 1–7, 2012, doi: 10.1155/2012/152385.

[28] Warju and I. M. Muliatna, "Environmental Friendly Innovative Muffler Design Using Metallic Catalytic Converter Technology to Support the Blue Sky Program (1st Year of Funding)," Surabaya, 2012.

[29] Warju and I. M. Muliatna, "Environmentally Friendly Innovative Muffler Design Using Metallic Catalytic Converter Technology to Support the Blue Sky Program (2nd Year of Funding)," Surabaya, 2013.

[30] S. D. Sulistiono and Warju, "Performance of Metallic Catalytic Converter Made from Nickel-Plated Brass Against Engine Performance, Reduction of Exhaust Emissions, and Noise Levels of Yamaha V-Ixion Motorcycles in 2011," Universitas Negeri Surabaya, 2014.

[31] E. W. Amboro and Warju, "The Effect of Using Metallic Catalytic Converter Made from Brass and Application of SASS Technology on Emissions of the Honda New Mega Pro Motorcycle," *Jurnal Teknik Mesin (JTM)*, vol. 1, no. 2, 2013.

[32] Warju, "Eco-Friendly Motorcycle Exhaust Products with Metallic Catalytic Converter Technology," Surabaya, 2017.

[33] Warju, A. N. F. Ganda, Suprayitno, and J.-C. Yu, "Robust Parameter Design Muffler Berteknologi Metallic Catalytic Converter dan Implementasinya untuk Mereduksi Emisi Gas Buang Dan Meningkatkan Performa Mesin Menggunakan Dual Response Surface Method," Surabaya, 2021.

[34] S. R. Ariyanto, R. Wulandari, Suprayitno, and P. I. Purboputro, "Pengaruh Metallic Catalytic Converter Tembaga Berlapis Chrome Dalam Menurunkan Emisi Gas Buang Mesin Sepeda Motor Empat Langkah," *Jurnal Media Mesin*, vol. 23, no. 1, pp. 44–51, 2022, doi: 10.23917/mesin.v23i1.16604.

[35] P. Bernard, P. Stelmachowski, P. Broś, W. Makowski, and A. Kotarba, "Demonstration of the Influence of Specific Surface Area on Reaction Rate in Heterogeneous Catalysis," *Journal of Chemical Education*, vol. 98, no. 3, pp. 935–940, Mar. 2021, doi: 10.1021/acs.jchemed.0c01101.

[36] H. Elçiçek, E. Akdoğan, and S. Karagöz, "The Use of Artificial Neural Network for Prediction of Dissolution Kinetics," *The Scientific World Journal*, vol. 2014, pp. 1–9, 2014, doi: 10.1155/2014/194874.

[37] S. Abirami and P. Chitra, "Energy-efficient edge based real-time healthcare support system," in *Advances in Computers*, 2020, pp. 339–368.

[38] P. Sahoo, "Tribological performance of electroless Ni-P coatings," in *Materials and Surface Engineering*, Elsevier, 2012, pp. 163–205.

[39] A. C. Mitra, M. Jawarkar, T. Soni, and G. R. Kiranchand, "Implementation of Taguchi Method for Robust Suspension Design," *Procedia Engineering*, vol. 144, pp. 77–84, 2016, doi: 10.1016/j.proeng.2016.05.009.

[40] K. G. Sheela and S. N. Deepa, "Review on Methods to Fix Number of Hidden Neurons in Neural Networks," *Mathematical Problems in Engineering*, vol. 2013, pp. 1–11, 2013, doi: 10.1155/2013/425740.

[41] K.-W. Lin and Y.-C. Chang, "Use of the Taguchi Method to Optimize an Immunodetection System for Quantitative Analysis of a Rapid Test," *Diagnostics*, vol. 11, no. 7, p. 1179, Jun. 2021, doi: 10.3390/diagnostics11071179.

[42] R. V. Aleksandrovich and G. Siamak, "The Effect of Tool Construction and Cutting Parameters on Surface Roughness and Vibration in Turning of AISI 1045 Steel Using Taguchi Method," *Modern Mechanical Engineering*, vol. 04, no. 01, pp. 8–18, 2014,

doi: 10.4236/mme.2014.41002.

[43] W. S. Alaloul and A. H. Qureshi, "Data Processing Using Artificial Neural Networks," in *Dynamic Data Assimilation - Beating the Uncertainties*, IntechOpen, 2020.

[44] M. H. Esfe, S. A. Eftekhari, M. Hekmatifar, and D. Toghraie, "A well-trained artificial neural network for predicting the rheological behavior of MWCNT–Al2O3 (30–70%)/oil SAE40 hybrid nanofluid," *Scientific Reports*, vol. 11, no. 1, p. 17696, Aug. 2021, doi: 10.1038/s41598-021-96808-4.

[45] A. Shafiq, A. Batur Çolak, T. Naz Sindhu, S. Ahmad Lone, A. Alsubie, and F. Jarad, "Comparative study of artificial neural network versus parametric method in COVID-19 data analysis," *Results in Physics*, vol. 38, p. 105613, Jul. 2022, doi: 10.1016/j.rinp.2022.105613.

[46] M. S. Umam, M. Mustafid, and S. Suryono, "A hybrid genetic algorithm and tabu search for minimizing makespan in flow shop scheduling problem," *Journal of King Saud University - Computer and Information Sciences*, Sep. 2021, doi: 10.1016/j.jksuci.2021.08.025.

[47] H. M. Pandey, "Performance Evaluation of Selection Methods of Genetic Algorithm and Network Security Concerns," *Procedia Computer Science*, vol. 78, pp. 13–18, 2016, doi: 10.1016/j.procs.2016.02.004.

[48] Y.-B. Li, H.-B. Sang, X. Xiong, and Y.-R. Li, "An Improved Adaptive Genetic Algorithm for Two-Dimensional Rectangular Packing Problem," *Applied Sciences*, vol. 11, no. 1, p. 413, Jan. 2021, doi: 10.3390/app11010413.

[49] X.-S. Yang, "Genetic Algorithms," in *Nature-Inspired Optimization Algorithms*, Elsevier, 2014, pp. 77–87.

[50] A. Sánchez-Chica, E. Zulueta, D. Teso-Fz-Betoño, P. Martínez-Filgueira, and U. Fernandez-Gamiz, "ANN-Based Stop Criteria for a Genetic Algorithm Applied to Air Impingement Design," *Energies*, vol. 13, no. 1, p. 16, Dec. 2019, doi: 10.3390/en13010016.

[51] R. S. Nursal, A. H. Hashim, N. I. Nordin, M. A. Abdul Hamid, and M. R. Danuri, "CFD analysis on the effects of exhaust backpressure generated by four-stroke marine diesel generator after modification of silencer and exhaust flow design," *ARPN Journal of Engineering and Applied Sciences*, vol. 12, no. 4, pp. 1271–1280, 2017.

[52] R. Fox, A. McDonald, and P. J. Pritchard, *Introduction to Fluid Mechanics*, 8th ed. John Wiley & Sons, Inc, 2011.

[53] SNI 09-7118.2-2005, *Exhaust gas emissions - Moving sources - Part 2: How to test motorized M, N, and O category vehicles with compression-ignition engine under free acceleration conditions*. Indonesia: National Standardization Agency (NSA).

[54] SAE J1349, *Engine Power Test Code-Spark Ignition and Compression Ignition-Net Power Rating*. Warrendale: SAE International, 2004.

[55] N. Gunantara, "A review of multiobjective optimization: Methods and its applications," *Cogent Engineering*, vol. 5, no. 1, p. 1502242, Jan. 2018, doi: 10.1080/23311916.2018.1502242.

[56] S. Khanmohammadi, O. Kizilkan, and F. Musharavati, "Multiobjective optimization of a geothermal power plant," in *Thermodynamic Analysis and Optimization of Geothermal Power Plants*, Elsevier, 2021, pp. 279–291.

[57] R. Kumar, R. Singh, I. S. Ahuja, and K. N. Karn, "Joining of 3D Printed Dissimilar Thermoplastics With Friction Welding: A Case Study," in *Encyclopedia of Renewable and Sustainable Materials*, Elsevier, 2020, pp. 97–108.

[58] N. Azri, R. Irmawati, U. I. Nda-Umar, M. I. Saiman, and Y. H. Taufiq-Yap, "Promotional effect of transition metals (Cu, Ni, Co, Fe, Zn)–supported on dolomite for hydrogenolysis of glycerol into 1,2-propanediol," *Arabian Journal of Chemistry*, vol. 14, no. 4, p. 103047, Apr. 2021, doi: 10.1016/j.arabjc.2021.103047.

[59] H. Li *et al.*, "Catalytic hydrogenation of maleic anhydride to γ-butyrolactone over a high-performance hierarchical Ni-Zr-MFI catalyst," *Journal of Catalysis*, vol. 410, pp. 69–83, Jun. 2022, doi: 10.1016/j.jcat.2022.04.011.

[60] V. V. Ranade and S. S. Joshi, "Catalysis and Catalytic Processes," in *Industrial Catalytic Processes for Fine and Specialty Chemicals*,

Elsevier, 2016, pp. 1–14.

[61] L. Piccolo, "Surface Studies of Catalysis by Metals: Nanosize and Alloying Effects," 2012, pp. 369–404.

[62] M. H. S. Morad, "Development of new highly active nano gold catalysts for selective oxidation reactions," University of Cardiff, 2014.

[63] I. Chorkendorff and J. W. Niemantsverdriet, *Concepts of Modern Catalysis and Kinetics*. Strauss Offsetdruck: Wiley-VCH, 2003.

[64] S. Dey and N. S. Mehta, "Selection of Manganese oxide catalysts for catalytic oxidation of Carbon monoxide at ambient conditions," *Resources, Environment and Sustainability*, vol. 1, p. 100003, Sep. 2020, doi: 10.1016/j.resenv.2020.100003.

[65] R. Flitney, "Materials," in *Seals and Sealing Handbook*, Elsevier, 2014, pp. 369–435.

[66] M. Bhandwal, M. Kumar, M. Sharma, U. Srivastava, A. Verma, and R. K. Tyagi, "The effect of using the turbulence enhancement unit before the catalytic converter in diesel engine emissions," *International Journal of Ambient Energy*, vol. 39, no. 1, pp. 73–77, Jan. 2018, doi: 10.1080/01430750.2016.1237889.